Optical dephasing and vibronic relaxation in molecular mixed crystals

Hesselink, Wim H.; Wiersma, Douwe A.

Link to publication in University of Groningen/UMCG research database

Optical dephasing and vibronic relaxation in molecular mixed crystals: A picosecond photon echo and optical study of pentacene in naphthalene and p-terphenyl

Wim H. Hesselink and Douwe A. Wiersma

Picosecond Laser and Spectroscopy Laboratory of the Department of Physical Chemistry, The University of Groningen, Nijenborgh 16, 9747 AG Groningen, The Netherlands

Picosecond photon echo and spectroscopic measurements have been used to establish that optical dephasing in the pure electronic and several vibronic transitions of pentacene in naphthalene is induced by pseudolocal phonon scattering in the ground and excited state. The frequency and low-temperature lifetime of this local phonon are 18 cm^{-1} and 3.5 ps in the groundstate and 13.8 cm^{-1} and 11 ps in the excited state (vibron independent). The deuterium isotope effect on the local phonon frequency demonstrates its molecular character and suggests its assignment as an in-plane librational mode. For the system pentacene in p-terphenyl photon echo measurements indicate the existence of a librational mode of $\simeq 30$ cm^{-1} with a $\simeq 1.5$ ps lifetime. Line shift measurements on both mixed crystal systems further show that the observed temperature induced shift is due to a difference in quadratic electron–bandphonon coupling of the ground and excited state and crystal anharmonicity (thermal expansion). We further report for a number of vibronic transitions the low-temperature dephasing times. Stimulated picosecond photon echo measurements are used to show that these relaxation times are only determined by population relaxation. No systematic variation is observed between the vibronic relaxation times and excess vibrational energy which indicates that the intramolecular anharmonic coupling determines the initial step in the vibrational energy dissipation process.

I. INTRODUCTION

In recent years it has become clear that pseudolocal modes (rotations, librations) are of crucial importance in a variety of relaxation phenomena. Brus and Bondybey[1] were the first to suggest that vibrational relaxation of small molecules as OH, OD, NH, and ND in rare gas lattices proceeds via transfer of vibrational energy into isoenergetic highly excited rotational levels. The role of the lattice phonons in this process is restricted to supplying energy compensating the mismatch.

Legay later showed[2] that in many small molecules the rotational mode acts as a doorway state in vibrational relaxation.

In the case of large organic molecules Aartsma and Wiersma,[3] studying photon echo relaxation in optical transitions of tetracene and pentacene in p-terphenyl, suggested that pseudolocal modes (hereafter named local phonons) played a dominant role in the optical dephasing process. The nature of these local modes however was not exposed. Gorokhovski and Rebane[4] supported this idea on basis of a photochemical hole burning study of a phtalocyanine derivative in solid tetradecane. Strong evidence for the dominant role of local phonons in optical dephasing was obtained by Voelker et al.[5] in a hole burning study of porphin in n-octane.

Verbeek et al.[6] studying spin-lattice relaxation in the lowest triplet state of naphthalene in durene also concluded that local phonons formed the dominant relaxation channels.

Despite these seemingly convincing cases, the role and nature of these local phonons in dephasing and relaxation of electronic (vibronic) transitions was being questioned.[7–9] One reason was that previous linewidth and shift measurements, at higher temperature, on optical

transitions by Burke and Small[10] could be satisfactorily explained on basis of the McCumber–Sturge theory,[11] whereby only coupling to the delocalized bandphonons is taken into account. In a recent paper by Hochstrasser and Nyi[9] it was shown that the linewidth and line shift data obtained on the system azulene in naphthalene could be explained on basis of either coupling to the delocalized bandphonons or coupling to local phonons. Another reason was that most of the results reported on optical dephasing, using the photon echo or hole burning technique, were obtained over a limited range of low temperatures and that therefore the validity of the proposed local-phonon-relaxation model at higher temperatures remained to be tested. Moreover, in many mixed crystals the identification of the local phonon corresponding to the observed activation energy remained problematic.

It therefore seemed highly desirable to extend the measurements of optical dephasing, using, e.g., the photon echo technique, up to higher temperature in order to test the validity of the proposed local-phonon-relaxation model.[12,13] With the success of Hesselink and Wiersma[14,15] to measure picosecond (ps) photon echo decay times such measurements have recently become feasible. In addition it seemed important to obtain more information on the nature of the local modes and to examine their possible role in vibrational relaxation of large molecules.

In this paper we report results of a detailed optical ps photon echo and stimulated photon echo study of the zero-phonon line and several vibronic transitions of pentacene in naphthalene and p-terphenyl. The results show that, up to 20 K, optical dephasing in the electronic and vibronic transitions is only caused by phonon scattering into a local mode in the ground and excited state.

In the pentacene in naphthalene system the local phonon
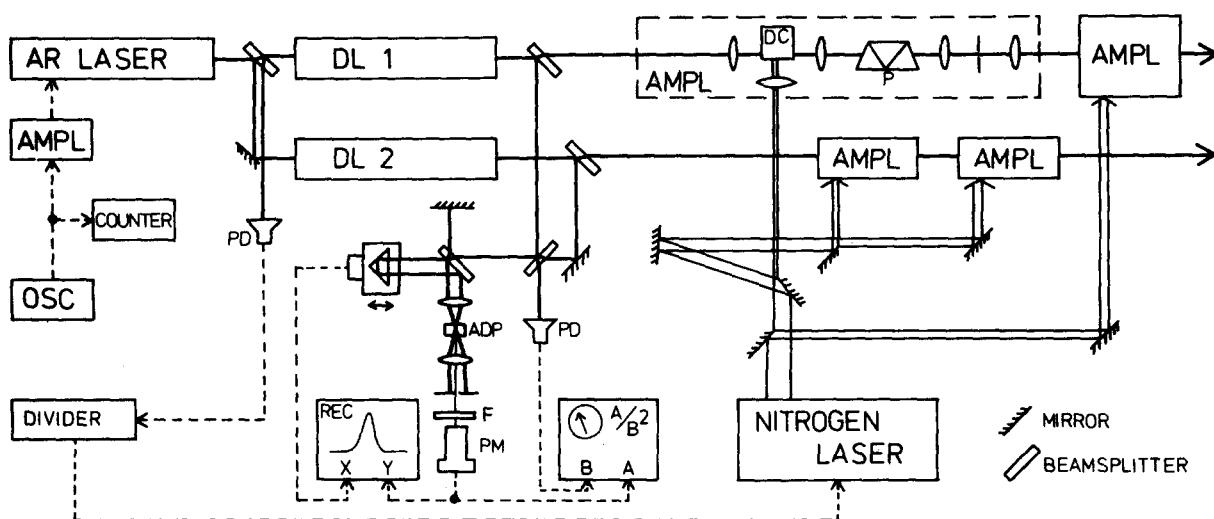
0021-9606/80/140648-16$01.00

FIG. 1. Schematic diagram of the dye laser system. Also shown is the interferometer used for measuring the autocorrelations and cross correlation. Solid lines are laser beams; dashed lines indicate electrical connections. PD: photodiode; PM: photomultiplier; F: Schott UG-5 filter; DC: dye cell; P: prism. Further details are described in the text and in Ref. 14.

is spectroscopically identified and on basis of a deuterium isotope effect assigned to an in-plane *librational* mode of the pentacene molecule. Our results further indicate that the ps lifetime of this librational mode is temperature dependent and considerably shorter in the ground state than in the excited state.

Line shift measurements suggest that for the system pentacene in p-terphenyl the shift is mainly due to a difference in quadratic electron–band phonon coupling of the ground and excited state.

In the pentacene in naphthalene system thermal expansion of the lattice mainly causes the line shift. From the low-temperature vibronic dephasing times, the vibrational relaxation times are calculated and no systematic variation in lifetimes versus excess vibrational energy is observed.

This paper is outlined as follows. In Sec. II the experimental setup is discussed. The necessary theoretical background to understand the formation and relaxation of the different kinds of photon echoes and the theories on optical dephasing is presented in Sec. III. The results and discussion are given in Sec. IV, while Sec. V contains conclusions.

II. EXPERIMENTAL

A. The laser system

The laser system, consisting of two synchronously pumped dye lasers followed by two amplifiers for each dye laser is shown in Fig. 1. Also shown is the interferometer used for measuring the autocorrelation and cross correlation by second harmonic generation. Details of this setup have been published previously.[14] Some changes and additional components will be mentioned here.

In the first place the pump laser for the amplifiers was replaced by a Molectron UV22 nitrogen laser. Synchronization of the nitrogen laser pulse with the dye

laser pulse train could now be maintained to ±1 ns. The use of a preionizer in the nitrogen laser almost eliminated long term drift. The probe laser (DL-2, a Coherent Radiation 590) was operated at 5570 Å in all experiments with sodium fluorescine (5×10^{-3}M in ethylene glycol) as active medium. The dispersive element was a three-element birefringent filter. With a 17% transmission output coupler this resulted in an autocorrelation width of 9 ps and a spectral width of 2.5 cm^{-1}. The excitation pulses were obtained from a Spectra Physics 375 dye laser (DL-1) containing Rhodamine 6G (1.5×10^{-3}M in ethylene glycol). Tuning was achieved with a two-element birefringent filter, in most experiments combined with an etalon. Output coupling was (10%–25)% depending on wavelength (increase to shorter wavelength). The resulting autocorrelation width at 5800 Å was 20 ps and spectral bandwidth was 1.2 cm^{-1} (4.3 ps and 7 cm^{-1} without etalon). Tuned to longer wavelength the pulse width increased and spectral width decreased (by ~25% at 6000 Å).

The lengths of the dye laser cavities were optimalized to the maximum of A/B^2,[16] where A is the second harmonic intensity and B is the fundamental power.

With this method a correction is made for the change in output power that occurs with tuning of the cavity length. The cross correlation width and relative timing of the two dye laser pulse trains reproduced very good after optimalization of the cavities in this way. Typically 21 ps cross correlation width (DL-1 with etalon) was observed corresponding to approximately 14 ps jitter between the dye lasers.

In the amplifiers of DL-1, Rhodamine (Rh) 110 was used in the experiments at 5767 Å; in the other experiments Rh 6G was used. The amplifiers of DL-2 contained sodium fluorescine. The concentration of all dyes used was 2.5×10^{-3}M in ethanol in the first amplifiers, while the second stages contained a solution of twice this concentration. The energy of the amplified excitation and probe pulse was 1 and 3 μJ, respectively.
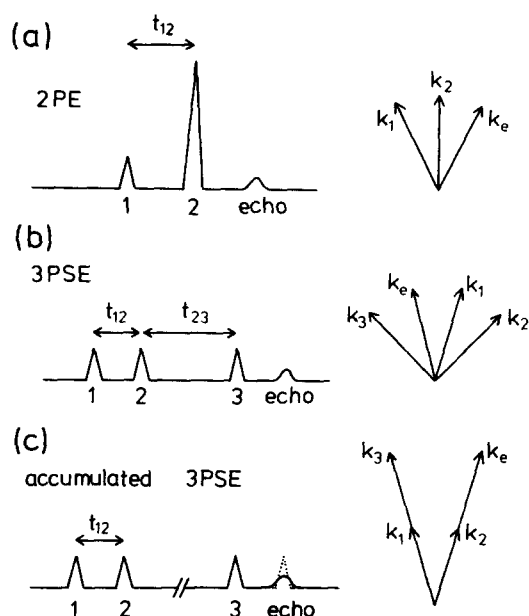
FIG. 2. Pulse cycles and phase matching conditions for the various types of photon echoes.

B. Photon echo experiments

The amplified excitation pulse was split and recombined by suitable beamsplitters to give the desired pulse cycle: two pulses with intensity ratio $1:4$ in a two pulse photon echo (2PE), three pulses with ratio $1:1:1$ in a three pulse stimulated photon echo (3PSE) experiment. The second (in a 2PE) or third (in a 3PSE) and the probe pulse could be delayed by translating stepper motor driven corner cubes. In a 2PE experiment the delay of the second excitation pulse was half of the probe pulse delay in order to maintain synchronization of the probe pulse with the echo. In a 3PSE experiment the delays were made equal. Maximum delay was 1.5 ns, so photon echo decay times of $\lesssim 1$ ns could be measured. The excitation pulses were focused on the sample by a 16 cm lens to a spot size of less than 100 μm. The photon echo emitted by the crystal, was optically mixed with the probe pulse[14] and detected via a Schott UG 11 color glass filter and a monochromator by a PM tube (EMI 9816 QB). When measuring short decay times it was necessary to reduce the background by spatially separating the echo from the excitation pulses. The parallel but noncollinear excitation pulses were focused on the sample at an angle of about 1.5°. The chosen wave vector geometries in the 2PE and 3PSE experiments are shown in Figs. 2(a) and 2(b). Spatial overlap was checked by focussing the pulses through a 100 μm pinhole mounted on the sample holder. The photon echo was passed through a diaphragm, which blocked the excitation pulses, and then mixed with the probe pulse. With this method the background was greatly reduced and decay times as short as 10 ps could be measured. In determining these short relaxation times, the tail of the echo decay curve is measured as the jitter limits the useful pulse separation. Note that the echo decay curve is still measured directly and that no deconvolution is required. The time resolution of the 3PSE is also 10 ps, for the chosen

wave vector geometry [Fig. 2(b)] enables decay measurements starting at $t_{23}=0$. After averaging with a boxcar integrator the echo signal was plotted on an X-Y recorder. The X axis was driven by a voltage proportional to the corner cube positions, so an echo decay curve was directly obtained.

In the accumulated 3PSE experiments,[17] the entire pulse train of one dye laser (DL-1) was used without amplification. The use of an intensity stabilizer was essential to obtain reliable relaxation times especially in the weaker vibronic transitions. The stabilized laser beam was split into two beams of equal intensity. One beam was modulated with a chopper at 300 Hz. The intensity of the other beam, which could be delayed, was phase sensitive detected with a PAR model 128 A lock-in amplifier after crossing the beams in the sample [Fig. 2(c)]. The resulting echo signal was superimposed on a background corresponding to a decrease in absorption due to a buildup of triplet state population.[18]

C. Phase matching

When excitation pulses with different k vectors are used in generating a photon echo, the echo amplitude is proportional to[19]

$$\left| \left(\sum_j \exp(i\Delta \mathbf{k} \cdot \mathbf{r}_j) \right)_{av} \right|^2 ,$$

which can be approximated by

$$f = \left| \frac{1}{l} \int_0^l \exp(i\Delta k r)\, dr \right|^2 = \frac{2}{(\Delta k l)^2}(1 - \cos \Delta k l) ,$$

where l is the sample length.

In all experiments described here the excitation pulses were polarized along the crystal b axis, which is a principal axis, so for the 2PE we find $\Delta k = |2k_2 - k_1 - k_e|$ $= (2n/\lambda)(1 - \cos \varphi)$, where φ is the angle between k_1 and k_2, n is the index of refraction along the b axis $[n = 1.72$ (Ref. 20)].

For our experimental conditions ($\lambda \simeq 6000$ Å, $\varphi = 1.5°$, $l = 1$ mm) this gives $\Delta k l = 1.96$ rad so $f = 0.72$. For the 3PSE we calculate $\Delta k l = 3.93$ and $f = 0.22$. This means that some intensity is lost by choosing noncollinear excitation pulses, but as the limiting factor in the echo experiments is background rather than intensity, it is in general advantageous to use the noncollinear geometry.

D. Sample preparation and spectra

Crystals were grown by the Bridgeman method from extensively zone refined naphthalene (B.D.H. "organic analytical standard") and p-terphenyl (Merck, "für Szintillation"). Pentacene (Fluka) was used without purification. Crystals were cut along the ab cleavage plane with a thickness of ~ 1 mm. Concentration was chosen such as to give $\sim 50\%$ absorption on the transition to be studied. Cryostate characteristics have been described previously.[3]

Absorption spectra were taken with a 1000 W Xe arc and 1 m Spex 1704 monochromator used in first order with a 1800 g/mm grating. The line positions were measured

by calibration of the spectrum with a Fe hollow cathode lamp. To avoid heating of the sample the light was passed through the monochromator first, so reliable temperature readings could be obtained. In the excitation spectra the total fluorescence was detected with a cooled EMI 9659 PM tube after filtering with Corning glass filters (2-58 or 2-60 depending on the wavelength).

E. Fluorescence lifetime

To determine the fluorescence lifetime of pentacene in naphthalene the electronic origin was excited using a nitrogen pumped dye laser (pulse width 5 ns). Fluorescence at 6569 Å was detected via a monochromator with a fast PM tube (RCA 7265) and displayed on a Tektronix transient digitizer. To avoid reabsorption only low concentration crystals were used (absorption less than 20% on the electronic origin).

III. THEORY

A. Photon echo formation

In this section we will summarize the decay characteristics and the directionality of the various types of photon echoes described in this paper. The major phenomena can be demonstrated in a simple two level system of which two cases will be considered: (a) a closed system in which the upper level decays into the nondecaying lower level. This is the situation in the pure electronic $S_0 \rightarrow S_1$ transition of pentacene; and (b) an open system, in which the upper level decays into other levels which have a long lifetime compared to the time scale of the experiment. This situation occurs in the experiments on vibronic transitions of the pentacene molecule as the decay times of interest in these experiments are much shorter than the lifetime of the pure electronic state. This state therefore acts as a bottleneck on a picosecond time scale.

The time development of the density matrix is given by

$$i\hbar \dot{\rho} = [H, \rho] + \cdots ,$$

where the dots represent relaxation terms and $H = H_0 - \mu \cdot E \cos(\Omega t - k \cdot r)$. In the rotating frame (indicated by tilde) this gives for the individual elements of the density matrix

$$\dot{\rho}_{22} = \frac{i\chi}{2} (\tilde{\rho}_{12} e^{-ik \cdot r} - \tilde{\rho}_{21} e^{ik \cdot r}) - \frac{\rho_{22}}{T_1} ,$$

$$\dot{\tilde{\rho}}_{12} = \frac{i\chi}{2} (\rho_{22} - \rho_{11}) e^{-ik \cdot r} + \left(i\Delta - \frac{1}{T_2}\right) \tilde{\rho}_{12} , \qquad (3.1)$$

$$\tilde{\rho}_{21} = \tilde{\rho}_{12}^* ,$$

$$\rho_{11} = 1 - \rho_{22} \quad \text{(case a)} ,$$

$$\dot{\rho}_{11} = \frac{i\chi}{2} (\tilde{\rho}_{21} e^{ik \cdot r} - \tilde{\rho}_{12} e^{-ik \cdot r}) \quad \text{(case b)} .$$

Here the terms $e^{ik \cdot r}$ are retained in the expressions to take the directionality of the echo into account. In Eq. (3.1), χ denotes the Rabi frequency, Δ is the detuning of the individual molecules due to the inhomogeneous broadening, T_2 is the phase relaxation time, and T_1 is the population relaxation time of the upper state. The ground state is assumed to be infinitely stable. The pure phase relaxation time T_2^* is related to T_2 by

$$T_2^{-1} = (T_2^*)^{-1} + (2T_1)^{-1} . \qquad (3.2)$$

Equations (3.1) can be compactly written

$$\dot{\rho} = iL\rho , \qquad (3.3)$$

where L is the Liouville operator.[21] The formal solution to Eq. (3.3) is simply

$$\rho(t) = e^{-iLt} \rho(0) . \qquad (3.4)$$

Making the usual assumptions of (i) resonant excitation and (ii) neglect of relaxation during excitation, the operator e^{-iLt} may be calculated, while the exciting pulses are on (A) and off (B) using Putzers method[22]

$$e^{-iL_A t} = \frac{1}{2} \begin{pmatrix} 1 + \cos\chi t & -i\sin\chi t\, e^{ik \cdot r} & i\sin\chi t\, e^{-ik \cdot r} & 1 - \cos\chi t \\ -i\sin\chi t\, e^{-ik \cdot r} & 1 + \cos\chi t & (1 - \cos\chi t)\, e^{-2ik \cdot r} & i\sin\chi t\, e^{-ik \cdot r} \\ i\sin\chi t\, e^{ik \cdot r} & (1 - \cos\chi t)\, e^{2ik \cdot r} & 1 + \cos\chi t & -i\sin\chi t\, e^{ik \cdot r} \\ 1 - \cos\chi t & i\sin\chi t\, e^{ik \cdot r} & -i\sin\chi t\, e^{-ik \cdot r} & 1 + \cos\chi t \end{pmatrix} , \qquad (3.5)$$

$$e^{-iL_B t} = \begin{pmatrix} 1 & 0 & 0 & 1 - e^{-t/T_1} \\ 0 & e^{(i\Delta - 1/T_2)t} & 0 & 0 \\ 0 & 0 & e^{(-i\Delta - 1/T_2)t} & 0 \\ 0 & 0 & 0 & e^{-t/T_1} \end{pmatrix} , \qquad (3.5a)$$

$$e^{-iL_B t} = \begin{pmatrix} 1 & 0 & 0 & 0 \\ 0 & e^{(i\Delta - 1/T_2)t} & 0 & 0 \\ 0 & 0 & e^{(-i\Delta - 1/T_2)t} & 0 \\ 0 & 0 & 0 & e^{-t/T_1} \end{pmatrix} . \qquad (3.5b)$$

It is then straightforward to calculate the echo intensities for the various pulse schemes by simple matrix multiplication and collection of the right terms. The photon echo amplitude can be shown[19] to be proportional to

$$\mathrm{Tr}\left[\mu_\rho(t)\right] = 2\mu_{12}\,\mathrm{Re}(\bar{\rho}_{12}\,e^{i\Omega t}) ,\qquad(3.6)$$

where μ_{12} is the transition dipole. This expression shows that the echo occurrence and decay is related to the off-diagonal element of the density matrix.

Using the Liouville operator technique leads for the 2PE to the well known results

$$I_e(2t_{12}) = I_e(0)\,e^{-4t_{12}/T_2} ,$$
$$k_e = 2k_2 - k_1 ,\qquad(3.7)$$

where t_{12} is the exciting pulse separation. These results apply to (a) closed as well as (b) open systems. For the 3PSE, one obtains

$$I_e(2t_{12} + t_{23}) = I_e(0)\,e^{-4t_{12}/T_2}e^{-2t_{23}/T_1} ,\qquad(3.8a)$$
$$I_e(2t_{12} + t_{23}) = I_e(0)\,e^{-4t_{12}/T_2}(e^{-t_{23}/T_1} + 1)^2\qquad(3.8b)$$
$$k_e = k_2 + k_3 - k_1 ,\qquad(3.8a, b)$$

where t_{23} is the separation between the second and the third pulse.

It follows from Eqs. (3.8) that in a closed system (a), the 3PSE decays with a single relaxation time $\frac{1}{2}T_1$ when t_{23} is varied. However, in the open system (b) the decay is more complex. Here the 3PSE exhibits a biexponential decay with decay times T_1 and $\frac{1}{2}T_1$ to a constant background. This background is due to the fact that the echo information, after two pulses, is stored in the population of the excited *and* the ground state. After two excitation pulses with areas θ_1 and θ_2 separated by time t_{12}, we have

$$\rho_{11} = \tfrac{1}{2}(1 + \cos\theta_1 \cos\theta_2 - \sin\theta_1 \sin\theta_2 \cos\Delta t_{12}\,e^{-t_{12}/T_2})$$
$$(t_{12} \ll T_1 , \quad k_1 = k_2) .\qquad(3.9)$$

The $\cos\Delta t_{12}$ modulation gives rise to the 3PSE when a third pulse is applied. So when there is no decay into the ground state, the modulation in ρ_{11} remains and the 3PSE can still be formed when ρ_{22} has vanished.

This phenomenon is also the basis of the accumulated 3PSE.[17] If the bottleneck in the relaxation path from $|2\rangle$ to $|1\rangle$ has a very long lifetime, buildup of the modulation in ρ_{11} can occur if a train of pairs of excitation pulses is used. Of course every excitation pulse also acts as a stimulating pulse [see Fig. 2(c)], analogous to the third pulse in a 3PSE, so a train of echoes is formed. The intensity of these echoes is proportional to the squared amplitude of the modulated part of ρ_{11} [in Eq. (3.9)] so we find for the accumulated 3PSE,

$$I_e(t_{12}) = I_e(0)\,e^{-4t_{12}/T_2} .\qquad(3.10)$$

Phase matching is the same as for the conventional 3PSE as given by Eqs. (3.8). When the wave vectors k_1 and k_2 are chosen as shown in Fig. 2(c) it follows that $k_e = k_2$. The echo is also time coincident with the second pulse of the next pair of excitation pulses. This means that, combined with the fact that the echo has the same
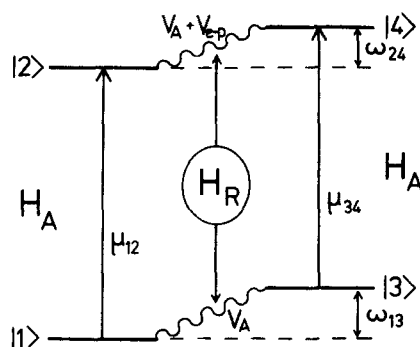

FIG. 3. Diagram of the four-level system. $|1\rangle$ and $|2\rangle$ are the ground and excited electronic states; $|3\rangle$ and $|4\rangle$ are the electronic states plus a local phonon.

phase[17] as the second excitation pulse, constructive interference between the echo and the probe pulse at the detector can occur. When the echo intensity is much less than the exciting pulse intensity the interference term is dominant and the echo *amplitude*, rather than the intensity, will be measured. This means that the decay time of the accumulated 3PSE is proportional to e^{-2t_{12}/T_2} in this phase matching geometry.

B. Dephasing theory

Several theories have recently been advanced to describe optical dephasing in molecular solids. For a review on the subject we refer to a paper by de Bree and Wiersma[13] (dBW) who also considered in detail, using Redfield relaxation theory, optical dephasing in molecular mixed crystals where localized phonons play a dominant role.

In this section we wish to briefly describe the highlights of this theory. The basic assumption in the dBW theory is that the localized phonons may be treated on equal footing with the electronic states. In the most simple relaxation model, shown in Fig. 3 two electronic states and two localized phonon levels in contact with a heat bath are considered. The Hamiltonian describing this situation is partitioned as follows. H_A describes the four levels (system), H_R the bath (the residual phonons), and V_{AR} the interaction between the levels and the bath. The precise form of these operators is given in Eq. (2.9) of Ref. 13.

An important point to note here is, as pointed out by Mukamel[23] that the initial choice of which levels are included in the system or bath, determines whether or not the calculated relaxation should be considered as a pure dephasing (T_2^*) or a population relaxation (T_1) process.

Using the Cohen–Tannoudji formulation of Redfield theory, dBW arrive at the following set of equations for the nondiagonal elements of the reduced density matrix of the system:

$$\dot{\rho}_{12} = -i\omega'_{12}\rho_{12} - \Gamma_{12}\rho_{12} + \Gamma_{34\text{-}12}\rho_{34} ,\qquad(3.11)$$
$$\dot{\rho}_{34} = -i\omega'_{34}\rho_{34} - \Gamma_{34}\rho_{34} + \Gamma_{12\text{-}34}\rho_{12} ,\qquad(3.12)$$

where ω'_{12} (ω'_{34}) is the normalized transition frequency, Γ_{12} (Γ_{34}) is the relaxation constant, and $\Gamma_{12\text{-}34}$ $(\Gamma_{34\text{-}12})$ is the

coherence transfer term. dBW showed that, unless the relation $|\omega'_{12} - \omega'_{34}| \lesssim \Gamma_{34-12}$ holds, coherence transfer among the transitions is negligible.

We wish to note here that Harris and co-workers[24] have used similar equations to describe vibrational dephasing through intermolecular exchange in polyatomic molecules. In their description the above relation was assumed to hold.

We will now examine the situation pertinent to pentacene in naphthalene, where coherence transfer is negligible (see Sec. IV. C). In this situation, Eqs. (3.11) and (3.12) are decoupled and in the absence of driving fields, the induced coherence at the optical transition (ρ_{12}) is expected to decay as

$$\rho_{12}(t) = \rho_{12}(0)\, e^{-\Gamma_{12}t} \ .$$

This expression shows that the photon echo intensity (I_{2PE}), which is related to ρ_{12} by the expression $I_{2PE} \sim |\mathrm{Tr}(\rho\mu)|^2$, is expected to decay with the rate constant $2\Gamma_{12}$.

The explicit expression for Γ_{12} is

$$\Gamma_{12} = \Gamma_{12}^A + \Gamma_{12}^{NA} \ , \tag{3.13}$$

$$\Gamma_{12}^A = \frac{\pi}{\hbar} \sum_\alpha p(\alpha) \sum_\beta \delta(E_\beta - E_\alpha)$$
$$\times \left| \langle \alpha 1 | V_{AR} | \beta 1 \rangle - \langle \alpha 2 | V_{AR} | \beta 2 \rangle \right|^2 \ , \tag{3.14}$$

$$\Gamma_{12}^{NA} = \tfrac{1}{2}(\Gamma_{1-3} + \Gamma_{2-4})$$
$$= \frac{\pi}{\hbar} \sum_{\alpha\beta} p(\alpha) \left| \langle \alpha 1 | V_{AR} | \beta 3 \rangle \right|^2 \delta(E_{\alpha 1} - E_{\beta 3})$$
$$+ \frac{\pi}{\hbar} \sum_{\alpha\beta} p(\alpha) \left| \langle \alpha 2 | V_{AR} | \beta 4 \rangle \right|^2 \delta(E_{\alpha 2} - E_{\beta 4}) \ , \tag{3.15}$$

where α and β are both heat bath states and $p(\alpha)$ is the occupation probability of heat bath state α. The effect of radiative and radiationless decay can be incorporated by adding appropriate decay constants to Γ_{12}.[13]

Equations (3.14) and (3.15) show that there are two distinctly different channels that contribute to optical dephasing in this model. The first one, denoted by Γ_{12}^A, is a pure dephasing (T_2^*) process, which is proportional to the difference of elastic phonon scattering processes in the ground and excited electronic state. In the Debye approximation for the band phonon density of states, this leads to an expression for Γ_{12}^A of the following form:

$$\Gamma_{12}^A = \bar\alpha \left(\frac{T}{T_D}\right)^7 \int_0^{T_D/T} \frac{dx\, x^6 e^x}{(e^x - 1)^2} \ , \tag{3.16}$$

where $\bar\alpha$ is a constant related to the difference of the average matrix elements

$$(\langle \alpha 1 | V_{AR} | \beta 1 \rangle - \langle \alpha 2 | V_{AR} | \beta 2 \rangle)$$

for all α and β, T_D is the lattice Debye temperature $(\hbar\omega_D/k)$ and $x = \hbar\omega/kT$.

At low temperature $(T \ll T_D)$, Γ_{12}^A then exhibits the well known T^7 temperature dependence as first derived by McCumber and Sturge.[11] The second process denoted by Γ_{12}^{NA} consists of two independent inelastic T_1-type phonon

scattering processes in the ground and excited state. In this process a local phonon state is populated at the expense of heat bath states. The precise mechanism of this phonon scattering mechanism depends on the explicit form of V_{AR}. It is clear however, that when the lifetimes of the local phonon levels in the ground and excited state, denoted by

$$\tau_3\, (\Gamma_{3-1}^{-1}) \quad \text{and} \quad \tau_4\, (\Gamma_{4-2}^{-1}) \ ,$$

respectively, are assumed to be constant in the temperature range of interest, Γ_{12}^{NA} will show a temperature dependence of the form

$$\Gamma_{12}^{NA} = \tfrac{1}{2}(\tau_3^{-1} e^{-\omega_{31}/kT} + \tau_4^{-1} e^{-\omega_{42}/kT}) \tag{3.17}$$

Here ω_{42} and ω_{31} denote the upper and lower state local phonon frequency, respectively.

In general both the elastic and inelastic scattering processes are expected to contribute to the coherence decay and optical line shape. In a certain temperature range one channel may of course be dominant.

The important results obtained may be summarized as follows.

Optical dephasing, and therefore the temperature dependence of the photon echo decay, is expected to show a T^7 low-temperature dependence in case elastic phonon scattering processes are most important. In case scattering via the local mode is the dominant dephasing channel, the photon echo decay as a function of temperature is expected to exhibit a biexponential activation. A special case occurs, when the local phonon frequencies in the ground and excited state are almost identical. In this situation optical exchange[24] may be important and the coupled equations (3.11) and (3.12) need to be solved. This situation is also discussed in detail in Ref. 13.

Recently, attempts have been made by Small[7] and Jones and Zewail[8] to modify the McCumber–Sturge theory in such a way that also an exponential activation of the echo relaxation time (line shape) is obtained, without invoking the presence of localized phonons. Instead of making the usual assumption of the McCumber–Sturge theory that all band phonons couple as efficiently, which leads to Eq. (3.16) for Γ_{12}, these authors assume preferential coupling to a density of states sharply peaked at a frequency ω_0. Γ_{12}^A is then found to be proportional to

$$\exp(\hbar\omega_0/kT)/[\exp(\hbar\omega_0/kT) - 1]^2 \ , \tag{3.18}$$

which at low temperature $(kT \ll \hbar\omega_0)$ leads to

$$\Gamma_{12}^A \sim \exp(-\hbar\omega_0/kT) \ . \tag{3.19}$$

We note here that, while this approach leads to an expression at low temperature for Γ_{12}^A formally similar to the one we obtain for Γ_{12}^{NA}, the results are not identical.

We first remark that the temperature dependence of the two dephasing rates at higher temperatures is different. The reason is that Eq. (3.18) is basically due to a Raman scattering process which is proportional to $\bar n(\omega_0)$ $\times [\bar n(\omega_0) + 1]$, whereby $\bar n(\omega_0)$ is the average phonon occupation number at ω_0. The temperature dependence of Eq. (3.17) on the contrary is only due to the assumption that
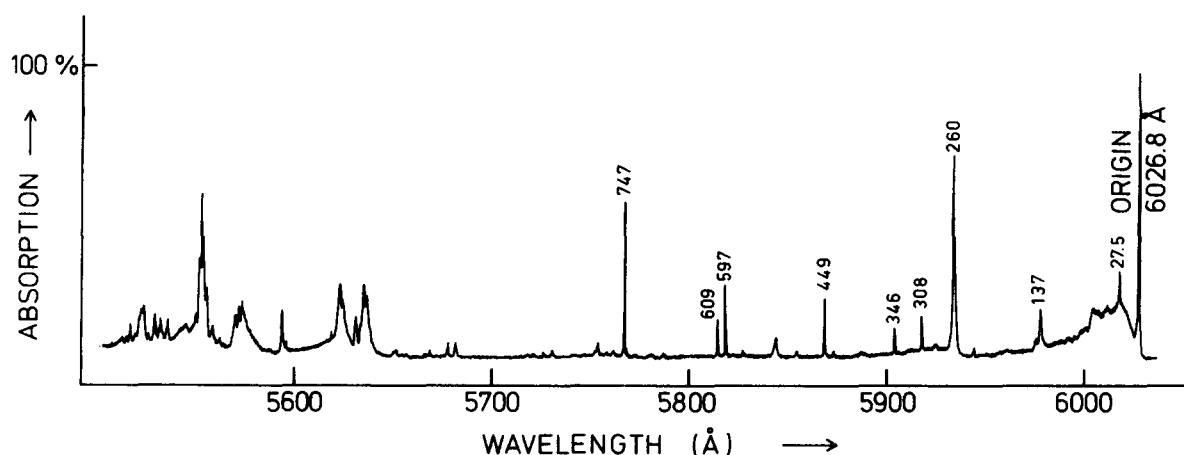
FIG. 4. Absorption excitation spectrum of pentacene in naphthalene at 1.5 K. The light was polarized along the crystal b axis. Indicated are the wavenumbers of the studied vibronic transitions compared to the electronic origin.

at every temperature the phonon upward scattering rate is related to the phonon lifetime ($\Gamma_{3\rightarrow 1}^{-1}$) by the Boltzman factor

$$\Gamma_{1\rightarrow 3} = \Gamma_{3\rightarrow 1} e^{-\omega_{31}/kT} .$$

A second point to note is that in the dBW theory the pre-exponential constants are directly interpretable as the local phonon lifetimes. This is not the case in the Small and Jones–Zewail approach.

A last point to recognize is that the dBW approach is more flexible and explicitly recognizes the special role of local phonons at the onset of the calculation. A prerequisite to application of this theory however is the spectroscopic identification of the local phonons.

We finally wish to emphasize the formal relationship that exists between the photon echo decay and the optical line shape. The general expression for the absorption line shape is[25]

$$I(\omega) \sim \int_{-\infty}^{\infty} dt\, e^{-i\omega t} \langle\langle \mu(0)\, \mu(t)\rangle\rangle , \qquad (3.20)$$

where ω is the photon frequency, μ is the transition dipole, and $\langle\langle\ \rangle\rangle$ denotes averaging over the initial ensemble states. We may further write,[26] for the unsaturated line shape,

$$\langle\langle \mu(0)\, \mu(t)\rangle\rangle = \langle \mu_{if}(0)\, \mu_{fi}(t)\rangle$$

$$= \mu_{if}(0)\langle \mu_{fi}(t)\rangle = \rho_{fi}(t)\,|\mu_{if}|^2 , \qquad (3.21)$$

where the fact is used that $\mu_{if}(0)$ is independent of the bath. Combining (3.20) and (3.21) leads to the requested result, namely,

$$I(\omega) \sim 2\,\text{Re} \int_0^{\infty} dt\, e^{i\omega t} \rho_{fi}(t) . \qquad (3.22)$$

This equation shows that the line width is determined by $\text{Re}[\rho_{fi}(t)]$.

In case of exponential decay of the photon echo, with lifetime T_2, the homogeneous width $\Delta\nu_L$ (FWHM) of the Lorentzian absorption line shape is given by the relation

$$\Delta\nu_L = (\pi T_2)^{-1} . \qquad (3.23)$$

IV. RESULTS AND DISCUSSION

A. Electronic spectrum

Figures 4 and 5 show the absorption–excitation spectrum of pentacene in naphthalene and in p-terphenyl at 1.5 K. Spectra were taken with the light polarized along the crystal b axis. In naphthalene only one site is present while in p-terphenyl, four sites of equal intensity are observed[27] and are labeled O_1 to O_4. Indicated in the spec-
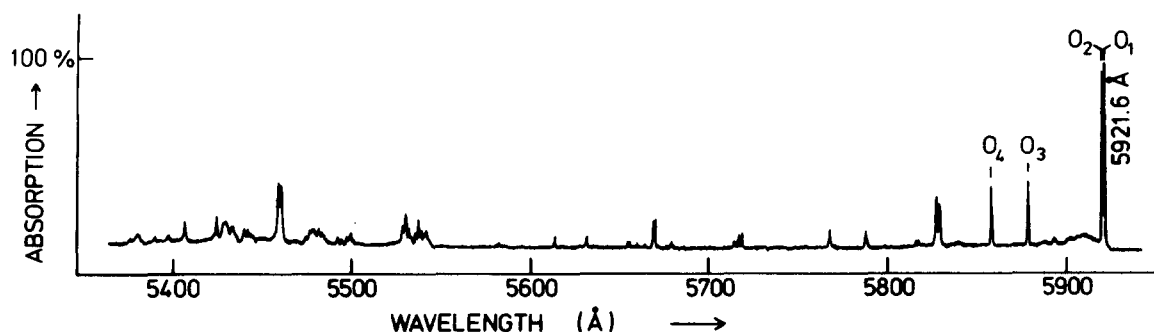

FIG. 5. Absorption excitation spectrum of pentacene in p-terphenyl at 1.5 K. The light was polarized along the crystal b axis. The O_3 and O_4 sites appear less intense than O_1 and O_2 due to spectral filtering of the emission. In a direct absorption experiment all four sites are observed with equal intensity.

tra are the studied vibronic transitions with their excess energy relative to the electronic origin (in wave numbers).

From pentacene in naphthalene also spectra were taken with the light polarized along the crystal a and c' axes. Absorption for these polarizations is approximately a factor 5 less, while no extra bands were observed. The direction cosines for pentacene in naphthalene, as measured by van Strien and Schmidt[28] with EPR methods are given in Table I. From the orientation of the molecule and the predominantly b-polarized spectrum it follows that the $^1B_{2u} - {}^1A_{1g}$ assignment for the electronic transition as was assumed previously,[27] is correct.

Spectra were also taken from the perdeuterated pentacene in naphthalene. All spectral data are summarized in Table II.

B. Phonon side band

1. Spectroscopy

Detailed absorption and emission spectra of the phonon side band of pentacene in naphthalene are shown in Fig. 6. Noteworthy in these spectra is the sharp feature at 27.5 cm^{-1} in absorption and the much broader band at $\simeq 36$ cm^{-1} in emission. This 27.5 cm^{-1} phonon was also observed in combination with the most intense vibronic bands (260 and 747 cm^{-1}). It will be shown in Sec. IV. C that the dephasing is exponentially activated, giving evidence for the existence of a localized phonon in this mixed crystal system. As this observed activation energy is approximately half the energy observed in the sideband spectra, we attempt to assign the bands in these spectra to transitions involving two quanta $(2 \leftarrow 0)$ of the local phonon mode. This assignment is substantiated by the observation at elevated temperature of a new band in the absorption spectrum 4.0 cm^{-1} to red of the zero phonon line as shown in Fig. 7. This band originates from the hot $1 \leftarrow 1$ transition.

We now have to explain the absence of the $1 \leftarrow 0$ transition. A simple explanation would be the assignment of u symmetry to the local phonon. However, for reasons given in the next section we believe that g symmetry is more likely. Now we can make two assumptions: (i) the local phonon can be described by a harmonic potential and (ii) the oscillator is not displaced upon excitation to the S_1 electronic state, only a change in frequency takes place. When these two conditions are satisfied, transi-

TABLE I. Direction cosines for pentacene in naphthalene[a] relative to the naphthalene crystal axes.

	a	b	c'
L	−0.390	0	+0.921
M	+0.360	+0.921	+0.153
N	−0.847	+0.391	−0.360

[a]Orientation of the translational not equivalent pentacene molecule is found by reflection in the ac' plane.

TABLE II. Spectral data of the pentacene $^1B_{2u} - {}^1A_{1g}$ transition.

| Pentacene-h_{14} in naphthalene		Pentacene-d_{14} in naphthalene	Pentacene-h_{14} in p-terphenyl
ν(vac cm^{-1})	Intensity[a]	ν(vac cm^{-1})	ν(vac cm^{-1})
16587.7 (o−o)	1.0	16613.4 (o−o)	16882.7 (o−o O_1)
16615.2 (+27.5)	0.013	16640.0 (+26.6)	16886.5 (o−o O_2)
16724.4 (+136.7)	0.036	16745.1 (+131.7)	17005.2 (o−o O_3)
16731.0 (+143.3)			17064.7 (o−o O_4)
16819.6 (+231.9)	≈0.002		
16848.1 (+260.4)	0.17	16866.0 (+252.6)	
16895.3 (+307.6)	0.012	16902.1 (+288.7)	
16934.1 (+346.4)	0.007	16928.1 (+314.7)	
16984.5 (+396.8)	≈0.004		
17036.2 (+448.5)	0.015	17028.8 (+415.4)	
17109.3 (+521.6)	0.016		
17160.1 (+572.4)			
17184.4 (+596.7)	0.024	17188.1 (+574.7)	
17196.8 (+609.1)	0.009	17203.6 (+590.2)	
17277.1 (+689.4)	0.001		
17331.1 (+743.4)			
17334.9 (+747.2)	0.044	17328.5 (+715.1)	
17350.6 (+762.9)			
17352.9 (+765.2)			
17376.5 (+788.8)			
17594.9 (+1007.2)	0.008		
17607.3 (+1019.6)	0.004		
17636.1 (+1048.4)	0.002		

[a]Relative to the o−o.
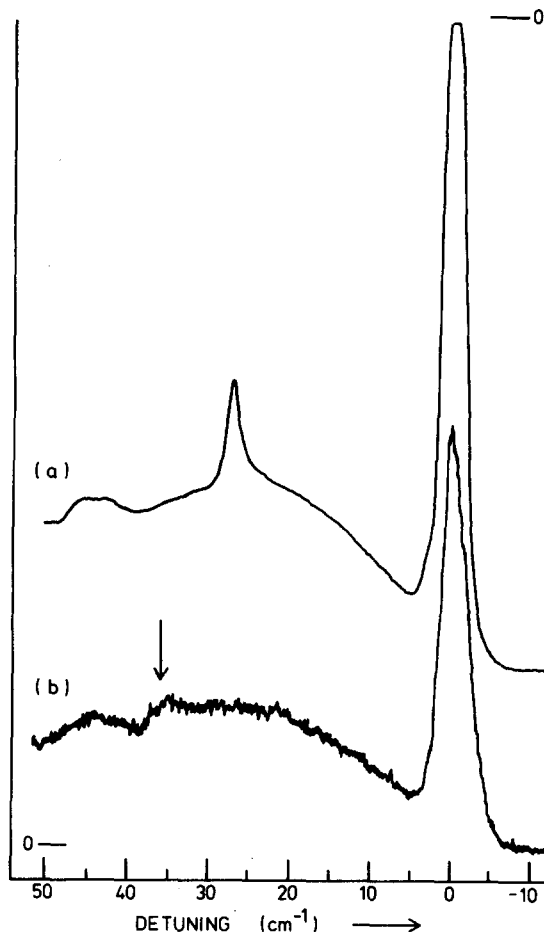
FIG. 6. Detailed absorption (a) and fluorescence (b) spectrum of the phonon side band of the origin of pentacene in naphthalene at 1.5 K. Note that in (a) the phonon side band is situated at higher energy, in (b) at lower energy relative to the zero phonon line. To facilitate comparison however they are plotted here in the same way. The intensity of the zero phonon line in emission is drastically reduced by the effect of reabsorption in this concentrated crystal.
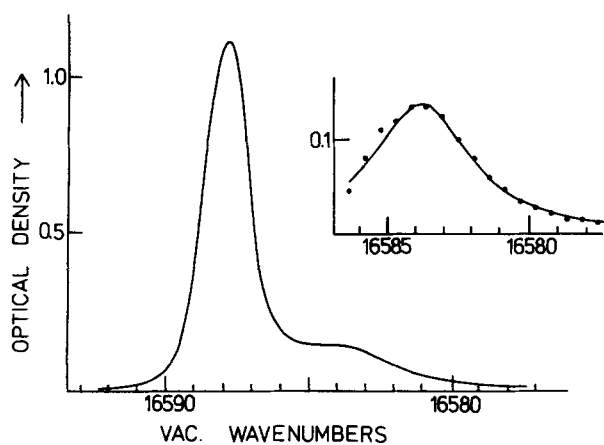
FIG. 7. Absorption spectrum of the zero phonon line of pentacene in naphthalene at 16 K. Inserted is the spectrum of the side band obtained by subtracting the main (0-0) peak from the spectrum. It was assumed that this 0-0 band is symmetrical. The solid line is a fit to a Voigt profile with $\Delta \nu_G = 2.0$ cm^{-1} and $\Delta \nu_L = 2.0$ cm^{-1}.

tions involving an odd number of quanta are forbidden so the $1 \leftarrow 0$ cannot be observed. Therefore we can explain the spectral features with a g-type harmonic mode of 18 cm^{-1} in the ground state reducing to 13.8 cm^{-1} in the excited state, but remaining harmonic.

From the linewidths in absorption and emission it is clear that the lifetime of the local phonon in the excited state is much longer than in the ground state. We will discuss this phonon lifetime in detail later on in connection with the dephasing (see Sec. IV.C).

In this picture it is straightforward to calculate the Franck-Condon factor of the $2 \leftarrow 0$ transition

$$f_{02} = \frac{(\omega_0 \omega_1)^{1/2}}{\omega_0 + \omega_1} \left(\frac{\omega_1 - \omega_0}{\omega_1 + \omega_0} \right)^2 = 0.009 .$$

Experimentally, we observe 0.010 relative to the zero phonon line combined with the acoustical phonon branch.

2. Nature of the local phonon

A first important point to note is the shift of the $2 \leftarrow 0$ absorption line upon deuteration of the pentacene molecule. This proves directly that the local phonon has to be considered as a *molecular* state and not as part of the host phonon branch. This also implies that one should consider in a theoretical description the local phonon as a well defined state as is done in the de Bree-Wiersma theory[13] of optical dephasing.

What can we say now about the nature of this local phonon? In principle, it could be either translational or rotational. Translational local (u-symmetry) phonons being of similar physical nature as the host acoustical ones are expected to strongly couple to these phonons resulting in a short lifetime or, stated otherwise, in a smeared-out delocalized state. Rotational-type local (g-symmetry) phonons (librations), however, are expected to survive coupling to the acoustic phonon branch and retain their identity. We, therefore, suggest that many of the sharp phonon side bands in the absorption and

emission spectra, named previously anomalous phonons,[29] are due to rotational oscillations of the guest molecule in a cage formed by the surrounding host molecules.

Local librational states of guest molecules will only occur when the guest librational frequency is outside the host optical branch. This implies that in isotopic mixed crystals local guest librations are not expected.

A beautiful example of a case where the rotational character of the local phonon could be shown presents the system Zn-porphin in n-heptane. Jansen *et al.*[30] demonstrated in an anti level crossing experiment between one of the Jahn-Teller components and a phonon side band not only that this phonon "belongs" to the molecule but also that its symmetry is consistent with a libration around the out of plane axis.

In the case of pentacene in naphthalene the only information on the nature of the local phonon comes from the isotope effect on its frequency. This effect is for a rotational-type phonon most likely due to a change in the moment of inertia. In Table III the results are given of a calculation of the moments of inertia for the pentacene molecule, when it rotates around the principal molecular axes.

For a free rotating molecule the rotational frequencies are expected to change by the factor $(I_H/I_D)^{1/2}$ upon deuteration. Comparison of the observed reduction value of 0.967 with the calculated ones suggests that the observed libration occurs either around the out of plane (N) or short (M) axis of the molecule. Additional experiments and calculations are necessary to discriminate between these possibilities.

C. Photon echo relaxation

1. Effect of limited inhomogeneous broadening

The linewidths of the absorption lines of pentacene in naphthalene and p-terphenyl are $\simeq 1$ cm^{-1}, which is approximately equal to the bandwidth of the exciting laser pulses. As these pulse are nearly transform limited the entire inhomogeneous line can be coherently excited. This is demonstrated in Fig. 8. Clearly the cross correlation of the photon echo with the probe pulse is much broader than the correlation between exciting and probe pulse. Taking the 8 ps probe pulse width and 13 ps jitter between the lasers into account the photon echo width is 33 ps.

Takeuchi[31] has shown that for pulse widths less than $0.7 * T_2'$, where T_2' defines the width of the Gaussian absorption line $G(\Delta\omega) = e^{-\Delta\omega^2 T_2'^2/2}$, the 2PE width (FWHM)

TABLE III. Moments of inertia for rotation about the principal molecular axes of pentacene-$h_{14}(I_H)$ and -$d_{14}(I_D)$.

	L axis	M axis	N axis
$I_H (* 10^{45}$ kg m$^2)$	6.22	69.7	76.1
$I_D (* 10^{45}$ kg m$^2)$	7.36	74.9	82.7
$(I_H/I_D)^{1/2}$	0.919	0.964	0.960

equals $2(\ln 2)^{1/2} T_2'$. From the observed 0.85 cm^{-1} inhomogeneous width of the absorption line we calculate the echo width to be 24.5 ps. The discrepancy with the measured value indicates that the inhomogeneous width of the volume of the sample, excited in the echo experiment, is less than that of the entire crystal, as measured in the absorption experiment. This difference in inhomogeneous width on different spots of the crystal was also observed in laser excitation spectra.

We note that this is the first time that in a photon echo experiment the full inhomogeneous linewidth is excited. The reported echo relaxation rates in the next sections therefore represent averaged rates over the inhomogeneous distribution of absorbing microsites.

2. Electronic origin of pentacene in naphthalene

The temperature dependence of dephasing in the electronic origin was studied with both the 2PE and the accumulated 3PSE method. All scans taken showed, within experimental error, a single exponential decay, so there is a well defined T_2. The fluorescence lifetime was measured to be 19.5 ± 1 ns independent of temperature up to 20 K. Also measurements of the 3PSE as a function of temperature confirmed that the shortening of T_2 is only due to dephasing processes. The T_1 value of 19.5 ns was used in Eq. (3.2) to obtain the pure dephasing time T_2^* from the observed T_2. Recently, Cooper et al.[32] observed that at low temperatures (1.5 K) not all dephasing processes are frozen out. They found $T_2 = 30$ ns instead of the expected 39 ns. This difference however has negligible effect on T_2^* in the temperature region of our experiments.

In Fig. 9, T_2^* as measured by the 2PE method is plotted on a logarithmic scale as a function of the inverse temperature. The data fit nicely to a straight line and can be described by the expression

$$T_2^*(T) = T_2^*(\infty) \exp(\Delta E/kT) ,$$

FIG. 9. Pure dephasing time T_2^* of the electronic origin of pentacene in naphthalene and in the O_1 site in p-terphenyl plotted as a function of the inverse temperature. Results were obtained in 2PE experiments. Solid lines are best fits assuming exponential activation with $\Delta E = 30$ cm^{-1}, $T_2^*(\infty) = 3.3$ ps (in p-terphenyl) and $\Delta E = 16.3$ cm^{-1}, $T_2^*(\infty) = 7.1$ ps (in naphthalene).

with $\Delta E = 16 \pm 1$ cm^{-1} and $T_2^*(\infty) = 7 \pm 2$ ps. We must keep in mind, however, that these values are only parameters used in fitting the experimental data and that they have not yet a clear physical meaning. Nevertheless they are very useful for comparing of results obtained for different transitions or crystals.

The T_2^* values calculated from the accumulated 3PSE experiments are shown in Fig. 10. From the low-temperature $(T \lesssim 10$ K) values, we obtain $\Delta E = 16 \pm 1$ cm^{-1} and $T_2^*(\infty) = 6.5 \pm 1.5$ ps, in agreement with the 2PE experiments. Due to the better time resolution of the accumulated 3PSE method, measurements can be made up to 20 K, where deviation from the simple exponential behavior is clearly visible.

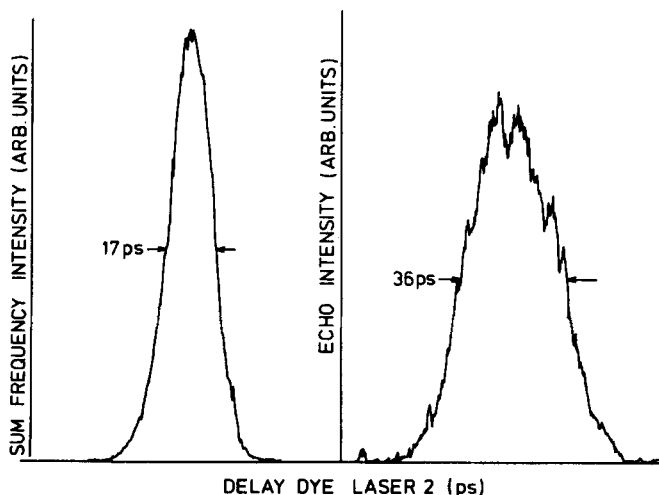We now turn to the discussion of these results taking

FIG. 8. Cross correlation between the excitation pulse and the probe pulse (left) and between the two pulse photon echo and the probe pulse (right). The photon echo was generated in the 0–0 of pentacene in naphthalene at 1.6 K with an excitation pulse separation of 116 ps.
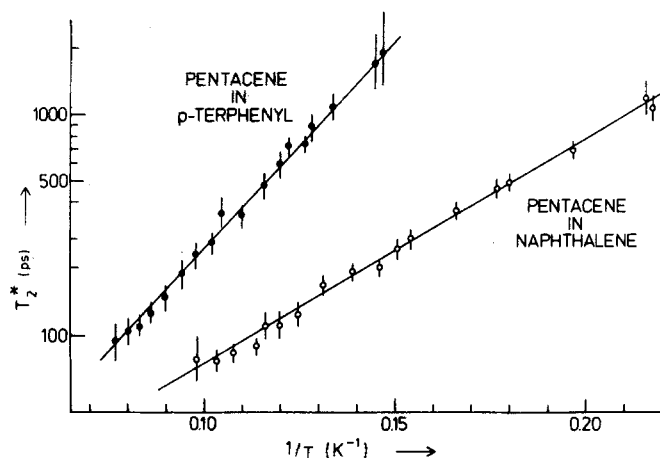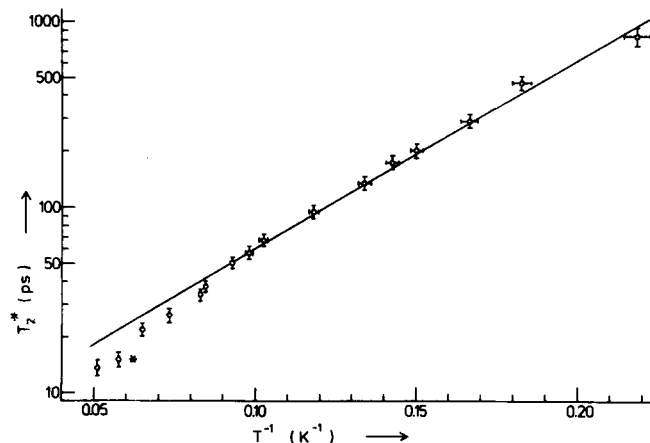
FIG. 10. Pure dephasing time T_2^* of the electronic origin of pentacene in naphthalene as a function of the inverse temperature. Results were obtained in accumulated 3PSE experiments. The solid line is calculated from Eq. (3.17) with $\omega_{13} = 18$ cm^{-1}, $\tau_3 = 3.5$ ps and $\omega_{24} = 13.8$ cm^{-1}, $\tau_4 = 11$ ps. The point at 16 K calculated with $\tau_3 = 2.2$ ps and $\tau_4 = 6.8$ ps as discussed in Sect. IV.C. is indicated with an asterisk.

into account the spectrally observed phonon frequencies. First we note that the zero phonon line ($0 \rightarrow 0$ in phonon quantum number) does not appreciably overlap with the $1 \rightarrow 1$ transition as can be seen from Fig. 7. This means that exchange contributions to the dephasing are negligible as now $\delta\omega T_{34\rightarrow12} > 1$. So dephasing can in this case be considered as the sum of the contributions from the ground and the excited state as given in Eq. (3.17). The two parameters left to adjust, once the frequencies are known, are the lifetimes of the local phonon in both electronic states. Fitting of the accumulated 3PSE data to Eq. (3.17) gives the curve drawn in Fig. 10, where $\tau_3 = 3.5$ ps ($\omega_{13} = 18$ cm^{-1}) and $\tau_4 = 11$ ps ($\omega_{24} = 13.8$ cm^{-1}). As can been seen from Fig. 10 the results fit very well for $T \lesssim 10$ K. So at 5 K the contributions to the dephasing from both phonons are approximately equal but at higher temperatures the ground state scattering becomes more important due to its shorter lifetime.

We note here that in a limited temperature range (e.g. 5–10 K) the curve calculated from Eq. (3.17) is almost equal to a single exponential with $\Delta E = 16$ cm^{-1} so one has to be careful in assigning an observed exponential activation to a *single* phonon scattering process.

We can now compare these phonon lifetimes with the observed spectral widths of the phonon side bands. In the first place the widths of the $2 \rightarrow 0$ absorption and emission bands confirm the point that the phonon in the excited electronic state has a longer lifetime than in the ground state. However no direct comparison with the photon echo results can be made as these bands correspond to overtones of the local phonon mode. On the other hand the high temperature $1 \rightarrow 1$ transition has a width due to both the ground and the excited state. From the 3.5 and 11 ps lifetimes we calculate a 2.0 cm^{-1} homogeneous width. To explain the observed 3.3 cm^{-1} width at 7.1 K we arrive at a 2.0 cm^{-1} Gaussian inhomogeneous contribution, using the tabulated values of the Voigt profile.[33] Although this is some 30% larger than the inhomogeneous width of the broadest vibronic transition, it seems possible that the phonon state is more sensitive to strain than the electronic or vibronic states. So the low temperature (5–10 K) dephasing results are consistent with the observed linewidth of the phonon side band.

We now turn to the higher temperature results (10–20 K), where a deviation from the calculated curve is observed. In this temperature region a definite broadening of the phonon side bands is observed, so obviously the assumption of constant phonon lifetimes is no longer valid. As we have no detailed information about the formal temperature dependence of the phonon lifetime we made no attempt to adjust Eq. (3.17). Nevertheless we can have a look at the agreement between dephasing and sideband linewidth at a fixed temperature. At 16 K the $1 \rightarrow 1$ transition has a width of 4.2 cm^{-1} (Fig. 7), which corresponds to a 3.2 cm^{-1} homogeneous contribution taking the low temperature 2.0 cm^{-1} inhomogeneous width into account. When both phonon lifetimes are shortened by the same fraction we arrive at $\tau_3 = 2.2$ ps and $\tau_4 = 6.8$ ps. This results in a calculated value of 15 ps for T_2^* (indicated in Fig. 10). This is somewhat shorter

than the observed value of $\simeq 18$ ps. This small discrepancy may be due to several factors. (i) The assumption of a temperature independent underlying inhomogeneous linewidth is questionable. (ii) The hot $1 \rightarrow 1$ transition is coupled to an additional dephasing channel (e.g., the hot $2 \rightarrow 2$ transition), in which case the lifetime of the phonon is longer than calculated from the linewidth.

We can thus conclude that the optical dephasing of the electronic origin up to 20 K can be completely described by a T_1-type scattering to a local phonon. This phonon has a different lifetime in the ground and excited electronic state. Furthermore, its lifetime shortens at higher temperature ($T \gtrsim 10$ K). This description implies also that pure dephasing processes (e.g., Raman-type scattering) are relatively unimportant in the pentacene in naphthalene system in the temperature range studied.

We now wish to comment on the lifetime of the pentacene librational mode. First we note that according to the dBW theory[13] the local modes are expected to decay through local phonon–band phonon anharmonic interactions. Bellows and Prasad recently showed[34] that for the librational modes in *pure* naphthalene this mechanism explains the observed temperature induced line broadening. In fact for the low-temperature in-plane librational mode of 57 cm^{-1} they deduce a lifetime of > 100 ps. We obtain for the corresponding pentacene librational mode of 18 cm^{-1} in the ground state a lifetime of 3.5 ps. Taking into account the fact that lower frequency phonons are expected to relax slower, we conclude that the phonon-induced anharmonicity of the pentacene libration exceeds that of the naphthalene host libration by, at least, a factor of 10. A direct study of the relaxation of the guest libration seems of interest.

3. Electronic origin of pentacene in p-terphenyl

The dephasing in the O_1 site of pentacene in p-terphenyl was studied with the 2PE method. Morsink et al.[35] showed that in this system at low temperature T_2 equals $2T_1$, so the 23.5 ns (Ref. 12) fluoresence lifetime was used in Eq. (3.2) to obtain the pure dephasing time T_2^*. Also in this system an exponential activation was found, as shown in Fig. 9, with $\Delta E = 30 \pm 2$ cm^{-1} and $T_2^*(\infty) = 3 \pm 1$ ps. We note here that the same parameters were obtained from our most recent low-temperature nanosecond photon echo relaxation measurements.[36]

No sharp structure was observed in the phonon sideband, either around this or twice this frequency. The value of $T_2^*(\infty)$ indicates that the phonon lifetimes in this system are shorter ($\simeq 1.5$ ps) than in the pentacene/naphthalene system. This would be expected from the higher phonon frequency and thus the higher density of acoustical phonon background states to which relaxation most likely occurs. This short lifetime implies that the absorption and emission bands involving phonon states may be broad and therefore not visible on the acoustical phonon branch.

We conclude therefore that the same phonon scattering mechanism as for pentacene in naphthalene is responsible for the observed dephasing.

TABLE IV. Summary of the photon echo results on the vibronic transitions of pentacene in naphthalene.

$\Delta\nu^a$ (cm^{-1})	$\frac{1}{2} T_2{}^b$ (ps)	Spectral linewidth (cm^{-1})	ΔE (cm^{-1})	$T_2^*(\infty)$ (ps)
0		1.0	16 ± 1	7 ± 2
137	2.3 ± 0.4	≈ 3.5		
260	2.4 ± 0.4	3.4		
308	19 ± 2	1.5		
346	8.5 ± 1	1.3		
449	15 ± 1.5	1.1	≈ 17	≈ 5
597	19.5 ± 1.3	1.4	19 ± 2	4 ± 1.5
609	59 ± 3	1.1	18 ± 2	5 ± 1.5
747	33 ± 1.5	1.2	17 ± 1	5 ± 1.5

^{a}Relative to the $o-o$. ^{b}At 1.5 K.

4. Vibronic transitions of pentacene in naphthalene

In this section we will focus attention to the temperature dependence of the dephasing in the vibronic transitions. The results concerning the vibronic relaxation will be discussed in Sec. IV.E.

Prior to discussing the obtained results, we note that in a previous letter[15] the pump–probe experiments on a vibronic transition were interpreted as population (T_1) relaxation measurements. In the meantime, however,[17] we have learned that these pump–probe experiments in fact are accumulated 3PSE (T_2) relaxation measurements. The interpretation of these experiments therefore is erroneous and revised in this section.

We now turn to a discussion of the results. The low-temperature (1.5 K) relaxation times T_2 of the studied vibronic transitions are given in Table IV. These results were obtained using the accumulated 3PSE. On the 747 cm^{-1} band also 2PE experiments were done yielding the same results.

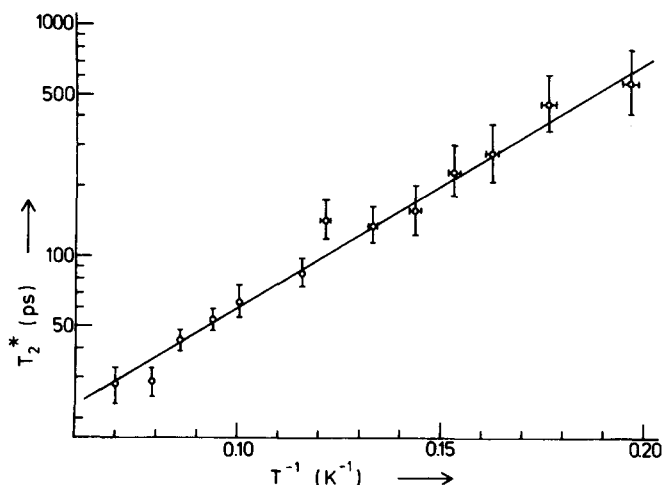The temperature dependent part of T_2 was defined,

FIG. 11. Pure dephasing time T_2^* of the 747 cm^{-1} vibronic transition of pentacene in naphthalene as a function of inverse temperature. The results were obtained in 2PE experiments. The solid line is a best fit of an exponential with $\Delta E = 16.6$ cm^{-1} and $T_2^*(\infty) = 5.4$ ps.
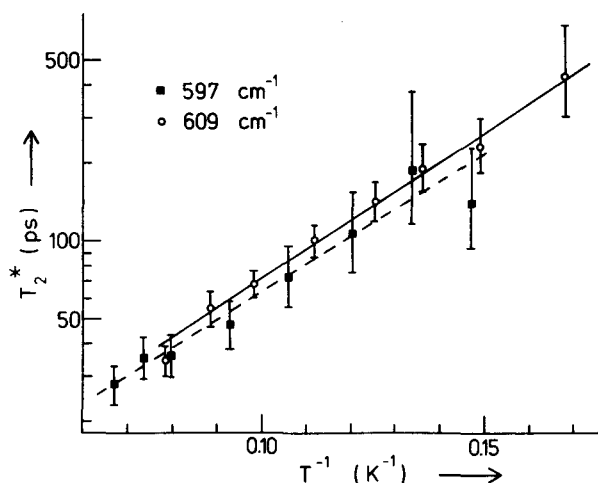
FIG. 12. Pure dephasing time T_2^* of the 597 and 609 cm^{-1} vibronic transitions of pentacene in naphthalene as a function of inverse temperature. Results were obtained using the accumulated 3PSE method. The solid line is a best fit to the data on the 609 cm^{-1} transition with $\Delta E = 18.3$ cm^{-1} and $T_2^*(\infty) = 5.2$ ps, the dashed line is a fit to the data on the 597 cm^{-1} transition with $\Delta E = 18.9$ cm^{-1} and $T_2^*(\infty) = 4.2$ ps.

analogous to Eq. (3.2) as $[T_2(T)]^{-1} = [T_2^*(T)]^{-1} + [T_2(1.5 \text{ K})]^{-1}$. In Figs. 11 and 12 the resulting values of $T_2^*(T)$ are plotted for several vibronic bands. Fitting of the data to an exponential results in the values for ΔE and $T_2^*(\infty)$ given in Table IV. The temperature dependence of the 449 cm^{-1} band was also studied, but ΔE and $T_2^*(\infty)$ could not be determined with great precision.

By comparison of these ΔE and $T_2^*(\infty)$ values with the results obtained on the electronic origin we note that they are approximately equal. The small differences can be accounted for by several reasons. First we concluded in the previous section that *two* scattering processes are active. This means that slightly different values of the parameters ΔE and $T_2^*(\infty)$ are obtained in different temperature regions. Also small differences in phonon frequency or lifetime cannot be excluded as we were not able to observe the phonon side bands in the weakest vibronic transitions. Furthermore, there could be some crystal dependence (see Sec. IV.C.5). Due to the large differences in oscillator strength between the origin and the vibronic bands we could not perform all experiments on the same crystal.

However, as the differences are small we conclude that the *same* processes are involved in dephasing of the different transitions and that the phonon frequencies and lifetimes differ little among the various vibrational states within the same electronic level.

Now two interesting conclusions can be drawn from this observation. (i) The variation in local phonon frequency for different vibronic levels, within the same electronic manifold, is caused by the difference in the diagonal *quartic* local phonon–vibron coupling. The observation of a vibron-independent local phonon frequency then implies a negligible contribution of this effect to the local phonon frequency. (ii) The vibron independence of the local phonon lifetime implies that also the *off*-diagonal
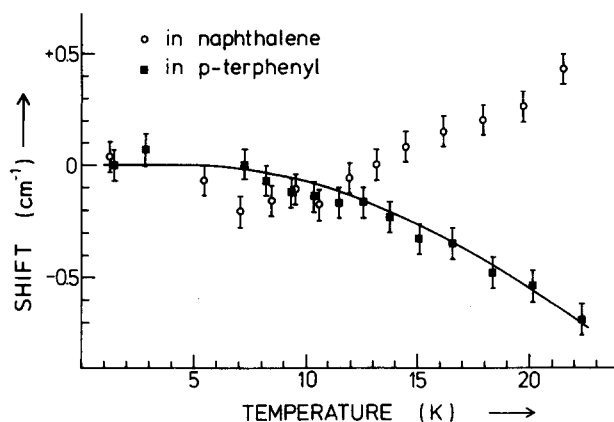
FIG. 13. Shift $[\nu(T)-\nu(0)]$ of the electronic origin of pentacene in naphthalene and in p-terphenyl as a function of temperature. The solid line is a fit of Eq. (4.2) to the data on pentacene in p-terphenyl with $\alpha = 17.5$ cm^{-1} and $T_D = 60$ K.

mixed quartic phonon–vibron coupling is small. The implication is that the local phonon is not expected to assist in the process of vibrational relaxation (redistribution). A general conclusion is that the separation between vibrations and librations, in a Born–Oppenheimer sense, for this pentacene electronic transition, is well justified.

This independence of thermal line broadening on vibronic level is not a universal feature; e.g., Burke and Small[10] found in 1, 3-diazaazulene and azulene in naphthalene a marked dependence on vibronic level which they ascribed to the influence of a quartic mixed vibron–phonon term in the hamiltonian.

There is in our results still one, seemingly surprising result: the fact that the 597 cm^{-1} vibronic band does not dephase by scattering to the nearby 609 cm^{-1} band. However, as the lifetime of the 609 cm^{-1} band is very long (59 ps) compared to the phonon lifetime, scattering to the phonon is much more efficient in the dephasing process.

Finally, we note that the equality of phonon frequencies in different vibronic levels indicates that for transitions within a given electronic level (e.g., Raman transitions) the exchange contribution to dephasing may be more prominent than in the electronic transitions described in this paper.

5. Sample dependence

Although all crystals used in this study were grown and handled in the same way, some crystal dependence on the relaxation was observed. In the first place the low temperature values of T_2 in the vibronic transitions varied in different crystals. These variations were very small (< 5%) and only just outside the experimental error. The numbers given in Table IV are averages over two or three crystals. Also the temperature dependence of T_2 in the vibronic bands as well as in the origin showed some crystal dependence. Here however variations occurred mostly in $T_2^*(\infty)$, while ΔE remained constant. Variations in $T_2^*(\infty)$ were ~ 20%.

D. Line shift

The spectral shift of the zero phonon line was determined by measuring the absorption spectrum as a function of temperature. The resulting values of the shift $\nu(T)-\nu(0)$ are shown in Fig. 13. Here $\nu(0)$ is the line position at low temperature (1.5 K) as given in Table II. The same crystals were used as in the 2PE decay measurements of Sec. IV.C. 2 and IV.C. 3. For pentacene in naphthalene we find initially a red shift (up to $\simeq 10$ K) and at higher temperatures a blue shift. This indicates that two opposing effects are determining the line shift. For pentacene in p-terphenyl only a red shift is observed.

There are several factors that may contribute to the observed line shift. First we note that in the previous section exchange was shown not to be important in the dephasing process in the electronic transition of pentacene in naphthalene and we therefore exclude this mechanism in both cases for the observed shifts. In the dBW paper on optical line shape,[13] a first order shift was calculated of the form

$$\Delta\omega_{f'f}(T) = \sum_K \left[(V_{KK}^{f'} - V_{KK}^{f})/\hbar \right] \bar{n}_K , \qquad (4.1)$$

where $\Delta\omega_{f'f}(T)$ is the line shift of the $\langle f' | \leftarrow | f \rangle$ transition, $\bar{n}_K$ is the average phonon occupation number, and $(V_{KK}^{f} - V_{KK}^{f})$ is the difference in the quadratic electron–band phonon coupling between the final and initial state. We note here that within the four-level relaxation model of dBW, the summation (4.1) over K excludes the local phonon. Assuming now a Debye density of states for the band phonons, the shift term may be expressed in the well known form first derived by McCumber and Sturge[11]

$$\Delta\omega_{f'f}(T) = \alpha \left(\frac{T}{T_D} \right)^4 \int_0^{T_D/T} \frac{x^3}{e^x-1} dx , \qquad (4.2)$$

where α is the average of the difference in quadratic electron phonon coupling in the excited and ground state, T_D is the Debye temperature $(\hbar\omega_D/k)$, and $x = \hbar\omega/kT$.

The solid line in Fig. 13 is a fit to the shift data for pentacene in p-terphenyl with $\alpha = 17.5$ cm^{-1} and $T_D = 60$ K. We conclude that the line shift in this system is determined by the electron-band phonon coupling mechanism. At this point we note that exchange seems to be excluded as mechanism for the lineshift, on basis of the broadening to shift ratio of $\simeq 1.5$.[13]

We interpret the initial low-temperature red shift in the system pentacene in naphthalene along the same line. The observed blue shift at higher temperature needs a different explanation. We propose that this blue shift is due to expansion of the crystal lattice with increasing temperature. Indeed it is well known that upon external pressure many zero phonon lines experience a red shift. In the case of pentacene in p-terphenyl at 2 K, Donnini[37] reported a 15 cm^{-1} red shift at an external pressure of 1 kbar. Sapozhnikov[38] has analyzed in some detail the observed zero phonon line shifts of a number of molecules in n-alkanes and shown that at 40 K, the line shift due to expansion of the lattice may easily amount to 0.05 cm^{-1}/K. This crystal-anharmonicity effect on the line shift may be quantitatively calculated[38] when the low-temperature thermodynamic data of the system are known. Pre-
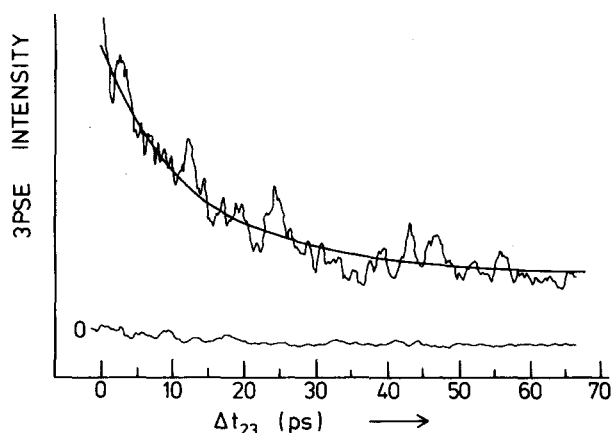
FIG. 14. Decay curve of the 3PSE on the 747 cm^{-1} vibronic transition of pentacene in naphthalene. The solid line is a fit of Eq. (3.8b) with $T_1 = 33$ ps.

sently not enough data are available to calculate the shift for the naphthalene crystal. The quoted data, however, show that the observed blue shift could easily be accounted for on basis of this mechanism. We further note that from our spectral and photon echo data on this system we have derived that the local phonon lifetime starts to become noticeably dependent on temperature above $\simeq 10$ K. As the local phonon lifetime is also dependent on the crystal anharmonicity it may not be so surprising that the anharmonicity effect on the lineshift also becomes important at this temperature.

At this point we note that the observed red shift in the system pentacene in p-terphenyl implies that the anharmonicity effect on the lineshift in this temperature range is hidden under the effect of electron—phonon coupling.

It is further interesting to realize that the gas-to-crystal shift of ~ 2000 cm^{-1} (Ref. 39) for pentacene in naphthalene is 300 cm^{-1} larger than for pentacene in p-terphenyl (O_1). This implies that the zero phonon lineshift of pentacene in naphthalene will be more affected by the thermal expansion of the lattice than in the case of pentacene in p-terphenyl.

In closing this section we note that in the system studied, the linewidth is determined by different processes than the shift. A similar situation was recently encountered by Bellows and Prasad[34] in a detailed analysis of the line shape of the optical phonons in pure naphthalene.

E. Vibrational relaxation

1. Cold relaxation

The measured low-temperature relaxation times on the vibronic transitions, as given in Table IV, are phase relaxation times so in principle they can contain a contribution from a pure dephasing process. However we can assume this contribution to be negligible for two reasons: (i) In the electronic origin no pure dephasing on a picosecond time scale was observed at low temperature. (ii) We measured the population lifetime T_1 in the 747 cm^{-1} vibronic band directly, using the 3PSE,

and the resulting value of T_1 was equal to $\frac{1}{2} T_2$. The experimentally observed 3PSE decay curve is shown in Fig. 14. As the S_1 electronic state acts as a bottleneck here, the curve was fitted to Eq. (3.8b). Good agreement was obtained with $T_1 = 33$ ps (solid line), the value measured in the low-temperature 2PE experiments. Note that the expected 4 : 1 ratio between the intensity at $t_{23} = 0$ and $t_{23} = \infty$ is actually observed. Here $t_{23} = 0$ corresponds to time coincidence of the second and third excitation pulses. Due to the chosen phase match geometry no background signal is observed. So we can conclude that the values tabulated in Table IV are the vibrational relaxation times.

Up until now there is no clear picture about the vibrational relaxation of large molecules. From gas phase fluorescence studies[40,41] it was concluded that large molecules exhibited ultra fast intramolecular energy redistribution. However these results were obtained from high temperature samples, where a large number of states is prepared due to the thermal population of ground state levels. Recently Jortner and co-workers[42] showed that low energy ($\lesssim 1000$ cm^{-1}) vibronic levels of tetracene and pentacene in a supersonic jet exhibited mostly unrelaxed fluorescene. Intramolecular energy redistribution is here apparently negligible.

Hochstrasser and Nyi[9] suggested on basis of hot emission spectra, observed in the system azulene in naphthalene, that an important vibrational decay channel in this case is the transfer of vibrational energy to host vibrational modes. For the system pentacene in naphthalene this mechanism seems unlikely in view of the measured hot emission spectra[43] which imply vibrational cascading in this system. Furthermore the observed guest isotope effect on vibrational relaxation[44] is in line with a dominant intramolecular contribution to this relaxation process.

For relaxation in the solid state Tamm and Saari[45] concluded from hot luminescence studies that in large molecules (e.g., perylene) the relaxation time shortenes with increasing vibrational energy. This would be due to the higher density of states to which relaxation can occur. For pentacene in naphthalene this is clearly not the case. There is no apparent relation between relaxation time and excess energy. This picture also emerges from a hole burning study by Voelker and Macfarlane[46] on porphin in n-octane.

So in systems where a single vibronic level can be excited, the relaxation seems to depend critically on the (unknown) structure of background levels to which relaxation can occur. Near resonance with other modes can lead to fast relaxation. In this respect it is surprising that the 609 cm^{-1} band of pentacene in naphthalene, which has a very long lifetime (59 ps) apparently only weakly couples with the nearby 597 cm^{-1} mode.

2. Hot relaxation

Presently little can be said about the relaxation at elevated temperatures. As announced in a previous note[15] we seem to observe in a 3PSE of the 747 cm^{-1} band of pentacene in naphthalene at higher temperature a shorten-

ing of the population relaxation time.

Unfortunately the experimental data obtained so far are not accurate enough to draw definite conclusions. We note therefore that the idea of local-phonon assisted vibrational relaxation of pentacene in naphthalene, as proposed in Ref. 15, cannot be confirmed by the experiments performed so far. This remains a point of further investigation.

V. EPILOG

In this paper the role of pseudolocal phonons (librations) in the process of optical dephasing for a specific system (pentacene in naphthalene) has been elucidated. The importance of this finding is that one may expect that in many mixed crystal systems, local guest librations are doorway states for optical dephasing.

The potential energy surface in different electronic states for these librations is expected to be different. As a consequence, the local phonon frequency may change appreciably on electronic excitation. Within an electronic manifold, the difference in local phonon frequency for various vibrations is only due to quartic anharmonic phonon–vibron interactions and is expected to vary less. We therefore conclude that exchange, involving local phonons, is a more likely mechanism for dephasing in vibrational than in electronic (vibronic) transitions.

This paper also shows that a completely satisfactory theoretical description of the dephasing process may be obtained using the Redfield relaxation theory of de Bree and Wiersma, where only the frequency and lifetime of the local phonon in ground and excited state determine the dephasing. We note here that modification of the well known McCumber–Sturge theory as suggested by Small and Jones and Zewail does not lead to a consistent interpretation of the *combined* spectroscopic and photon echo results. The modified McCumber–Sturge theory essentially fails to recognize the "molecular" character of the observed sharp phonon sidebands.

This paper further shows that the line shift and optical dephasing of the zero phonon line of pentacene in naphthalene are unrelated. We expect this to be the case in all optical transitions where exchange is unimportant.

This paper also reveals, not unexpectedly, that the local phonon lifetime shortens at higher temperature. We plan to investigate this point further in a picosecond CARS echo study of a suitable mixed crystal system.

Finally, this paper reports the first *direct* measurement of a number of vibrational lifetimes in the excited state of a large molecule. The seemingly random variation in measured vibrational lifetimes as a function of excess vibrational energy suggests intramolecular anharmonic vibration–vibration coupling to be of great importance. Interpretation of these results however must await detailed information on molecular background states and results of more experiments on similar systems.

[1]L. Brus and V. E. Bondybey, J. Chem. Phys. **63**, 786 (1975).
[2]F. Legay, in *Chemical and Biochemical Applications of Lasers*, Vol. II, edited by C. B. Moore (Academic, New York, 1977).
[3]T. J. Aartsma and D. A. Wiersma, Chem. Phys. Lett. **42**, 520 (1976).
[4]A. A. Gorokhovski and L. A. Rebane, Opt. Commun. **20**, 144 (1977).
[5]S. Voelker, R. M. Macfarlane, and J. H. van der Waals, Chem. Phys. Lett. **53**, 8 (1978).
[6]P. F. J. Verbeek, C. A. van 't Hof and J. Schmidt, Chem. Phys. Lett. **51**, 292 (1977).
[7]G. J. Small, Chem. Phys. Lett. **57**, 501 (1978).
[8]K. E. Jones and A. H. Zewail, *Advances in Laser Chemistry*, edited by A. H. Zewail (Springer, New York, 1978), p. 196.
[9]R. M. Hochstrasser and C. A. Nyi, J. Chem. Phys. **70**, 1112 (1979).
[10]F. P. Burke and G. J. Small, Chem. Phys. **5**, 198 (1974); J. Chem. Phys. **61**, 4588 (1974).
[11]D. E. McCumber and M. D. Sturge, J. Appl. Phys. **34**, 1682 (1963).
[12]T. J. Aartsma, J. B. W. Morsink, and D. A. Wiersma, Chem. Phys. Lett. **47**, 425 (1977).
[13]P. de Bree and D. A. Wiersma, J. Chem. Phys. **70**, 790 (1979).
[14]W. H. Hesselink and D. A. Wiersma, Chem. Phys. Lett. **56**, 227 (1978).
[15]W. H. Hesselink and D. A. Wiersma, Chem. Phys. Lett. **65**, 300 (1979).
[16]C. V. Shank and E. P. Ippen, Appl. Phys. Lett. **24**, 373 (1974).
[17]W. H. Hesselink and D. A. Wiersma, Phys. Rev. Lett. **43**, 1991 (1979).
[18]W. H. Hesselink and D. A. Wiersma, J. Chem. Phys. (to be published).
[19]I. D. Abella, N. A. Kurnit, and S. R. Hartmann, Phys. Rev. **141**, 391 (1966).
[20]K. S. Sundararajan, Z. Kristallogr. **93**, 238 (1936).
[21]W. G. Breiland, M. D. Fayer, and C. B. Harris, Phys. Rev. A **13**, 383 (1976).
[22]E. J. Putzer, Am. Math. Month. **73**, 2 (1966).
[23]S. Mukamel, Chem. Phys. **31**, 327 (1978).
[24]C. B. Harris, R. M. Shelby, and P. A. Cornelius, Phys. Rev. Lett. **38**, 1415 (1977).
[25]R. Kubo, J. Phys. Soc. Jpn. **12**, 570 (1957).
[26]S. Mukamel, Chem. Phys. **37**, 33 (1979).
[27]J. H. Meyling and D. A. Wiersma, Chem. Phys. Lett. **20**, 383 (1973).
[28]A. J. van Strien and J. Schmidt, Chem. Phys. Lett. **70**, 513 (1980).
[29]A. B. Zahlan, Proceedings of the Conference on Excitons Magnons, and Phonons in Molecular Crystals, Beirut (Cambridge University, 1968), p. 153.
[30]G. Jansen, M. Noort, G. W. Canters, and J. H. van der Waals, Mol. Phys. **35**, 283 (1978).
[31]N. Takeuchi, IEEE J. Quantum Electron. QE-11, 230 (1975).
[32]D. E. Cooper, R. W. Olson, and M. D. Fayer, J. Chem. Phys. **72**, 2332 (1980).

[33]D. W. Posener, Aust. J. Phys. **12**, 184 (1959).

[34]J. C. Bellows and P. N. Prasad, J. Chem. Phys. **70**, 1864 (1979).

[35]J. B. W. Morsink, T. J. Aartsma, and D. A. Wiersma, Chem. Phys. Lett. **49**, 34 (1977).

[36]T. J. Aartsma, thesis (University of Groningen, 1978) (unpublished).

[37]J. M. Donnini, J. Chim. Phys. **71**, 1543 (1974).

[38]M. N. Sapozhnikov, J. Chem. Phys. **68**, 2352 (1978).

[39]A. Amirav, U. Even, and J. Jortner, J. Chem. Phys. (to be published).

[40]S. Okajima and E. C. Lim, Chem. Phys. Lett. **37**, 403 (1976).

[41]B. Kopainsky and W. Kaiser, Chem. Phys. Lett. **66**, 39 (1979).

[42]A. Amirav, U. Even, and J. Jortner, J. Chem. Phys. **71**, 2319 (1979).

[43]A. van der Ende and R. P. H. Rettschnick (unpublished results).

[44]W. H. Hesselink and D. A. Wiersma, J. Chem. Phys. (to be published).

[45]T. Tamm and D. Saari, Chem. Phys. **40**, 311 (1979).

[46]S. Voelker and R. M. Macfarlane, Chem. Phys. Lett. **61**, 421 (1979).